Biogenic synthesis of Ag-ZnO hybrid nanocomposites and study of its photocatalytic, antifungal, antibacterial and cytotoxic activities.

Mrinalini Parmar[1], Vipul P. Patel[2], Girish Kashid[3], Brij Bhushan Santosh Pandey[4], Mallika Sanyal[5]
[1]*Department of Chemistry, Gujarat Arts and Science college, Gujarat University, Ahmedabad, Gujarat-380009, India*
[2] *Sanjivani college of Pharmaceutical Education and Research, Kopragaon, Ahmadnagar, Maharashtra-423603, India*
[3]*St. Xavier's College, Navrangpura, Ahmedabad, Gujarat-380009, India*

Graphical Abstract

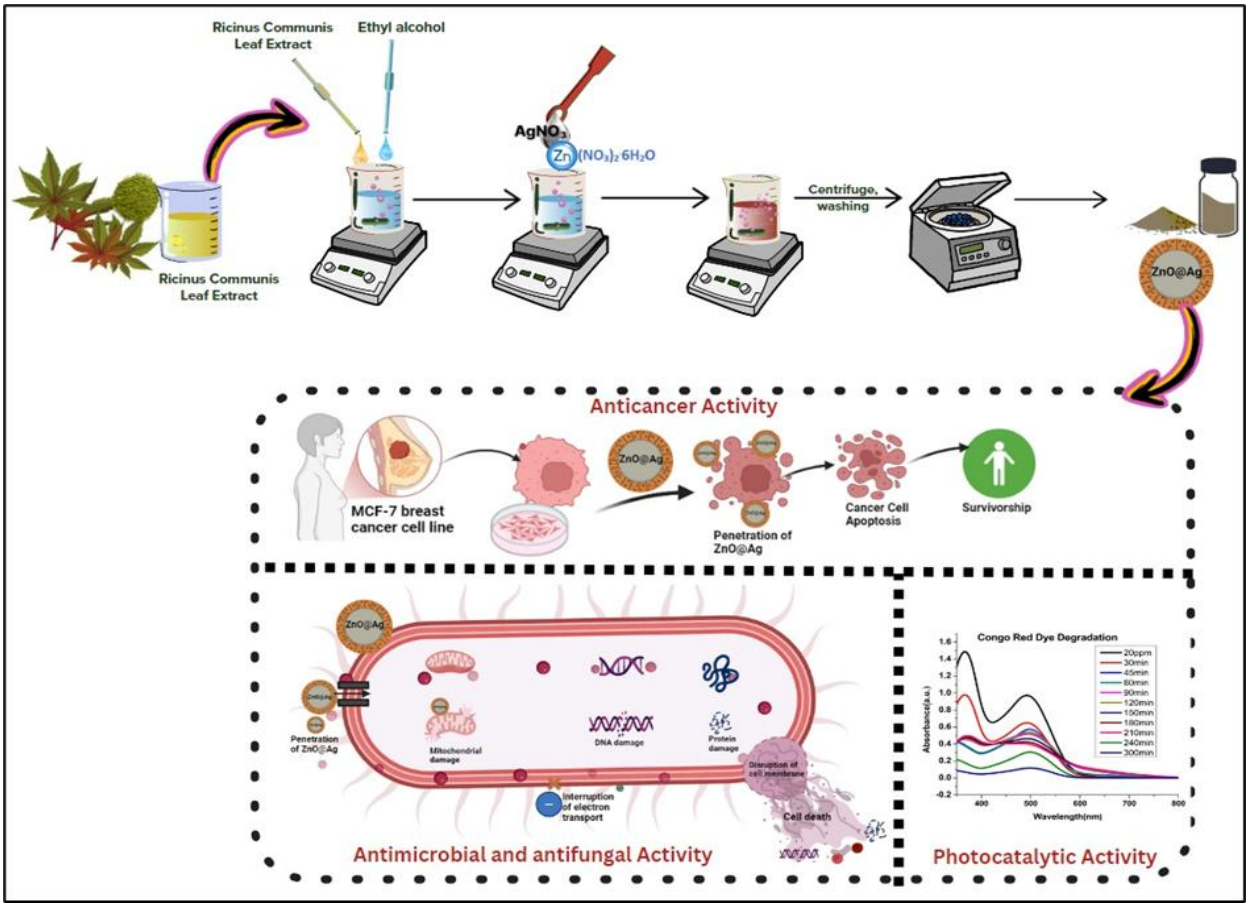

***Abstract*—In the present study, Ag–ZnO hybrid nanocomposites were biosynthesized using aqueous leaf extract of Ricinus communis. The formation of the nanocomposite was confirmed through X-ray diffraction (XRD), Fourier transform infrared spectroscopy (FTIR), energy-dispersive X-ray spectroscopy (EDX), and transmission electron microscopy (TEM) analyses. The average particle size of the synthesized nanocomposite was found to be approximately 21 nm. The photocatalytic activity of the biosynthesized Ag–ZnO nanocomposite**

was evaluated through degradation of Congo Red dye, achieving 88% degradation within 5 hours under irradiation. The biological applications of the nanocomposite were assessed by investigating its antifungal, antibacterial, and cytotoxic activities.
Antifungal activity was evaluated against Candida albicans (IC_{50} = 71.6 µg/mL) and Aspergillus fumigatus (IC_{50} = 132.1 µg/mL). Antibacterial activity was tested against Pseudomonas aeruginosa, Staphylococcus aureus, Escherichia coli, and Bacillus subtilis. The minimum inhibitory concentration (MIC) for P. aeruginosa was 6.25 µg/mL, which was lower than that observed for the other bacterial strains. Furthermore, cytotoxicity studies against the MCF-7 breast cancer cell line indicated significant anticancer potential of the synthesized nanocomposite.

***Index Terms*—Ag-ZnO NPs, Dye Degradation, Antifungal activity, Antibacterial activity, Cytotoxic activity**

I. INTRODUCTION

The sustainable development goals (SDGs) clearly emphasise on the need of clean drinking water and sanitation for human survival. Water borne diseases are a major cause of deaths worldwide. Providing clean water has now become an essentiality Nanoparticles in the form of metals and their composites have gained attention over the past decade in the scientific research arena due to its variable potential in a large number of fields (Ashna et al., 2022) (Amiri et al., 2021). The biomedical applications have led to new paths leading towards the use of nanomedicine and drug delivery in medical science (Hashemzadeh et al., 2021) (Parmar & Sanyal, 2022). The metal oxides and their doped counterparts prove to be of great use as sensors, electronics (Hameed et al., 2019), catalysis (Ahmad et al., 2021), energy storage devices (Ismail et al., 2016), magnetic resonance imaging, gas sensing (Khan et al., 2018) and medicine (Shunmuga Priya et al., 2021). Metals like Silver have a long history of around 5000 years for being a bactericidal agent. Silver nanoparticles serve as an excellent candidate for use in medical instruments, textiles and disinfectants (Parmar et al., 2023). They also provide potent cytotoxicity effects by releasing Ag+ ions from Ag Nanoparticles leading to apoptosis through mitochondrial pathway (Akter et al., 2018). Despite all these properties they have a limitation of forming aggregations when size of nanoparticles is very small leading towards reduced antibacterial activity. Hence to enhance its properties it must be either coated with a metal oxide like magnesium oxide, Calcium oxide, Zinc oxide or some polymer to produce core-shell model (Mtavangu et al., 2022a).

Various metal oxides have been studied in recent times for particularly good cytotoxicity, antifungal and antibacterial activities. Among them ZnO is a versatile oxide which exhibits both semiconducting as well as piezoelectric properties. It is a wide bandgap semiconductor having high exciton energy of 60 meV. Its high stability and low toxicity have led to its application in UV screening materials (Noohpisheh et al., 2020). They have shown excellent activity against both gram positive and gram-negative bacteria. They are known to supress the bacterial activity by either cell penetration or adhesion to the surface of the bacteria and production of ROS (Reactive Oxygen Species). Thus, synergising the combined activities of Silver and Zinc oxide, Ag-ZnO nanocomposites can be synthesised for better biological activities. So far various methods have been used for synthesis of Ag-ZnO nanocomposites, for example microwave radiation (Kundu et al., 2012), sol gel method (Ouarez et al., 2018), co-precipitation (Okumura et al., 2015), chemical vapour deposition (Haldar et al., 2018)and solvothermal (Pung et al., 2010)and so forth. All these methods require hazardous chemicals and produce toxic by-products. The need to maintain certain reaction conditions makes these procedures more cumbersome compromising the environment safety on one hand and increasing cost of production on the other (Biswas et al., 2021). Among all these procedures, the biogenic synthesis of nanoparticles using biomass is the easiest method which is environment friendly and cost effective at the same time [Au](Parmar & Sanyal, 2024). Selvan et.al have used Murraya koenigii and Zingiber officinale plant extracts for preparation of Ag-ZnO nanocomposites. Abutilon indicum, Clerodendrum infortunatum and Clerodendrum inerme extracts have also been used to prepare ZnO and Cu doped ZnO nanocomposites (Khan et al., 2018).
In the present study we have used Ricinus cumminis as a biofuel for synthesis of Ag-ZnO nanocomposite. Ricinus cumminis is a member of Euphorbiaceous family and is native to India. The shrub is cultivated

both annually and perennially throughout the country. It has medicinal properties as fresh juice of its leaves is used in treatment of jaundice and as an emetic in case of poisoning by narcotics. The oil produced from leaves is mainly used as a laxative (Jena et al., n.d.). The phenolic content of the leaves is mainly Rutin, quercetin, epicatechin, gentisic acid, gallic acid and ellagic acid. These act as reducing and capping agent for the formation of stable Nanocomposites (Singh et al., 2009).

II. MATERIALS AND METHODS

2.1 Materials:

Ricinus cummunis (Castor) leaves were collected from a local farm. Silver nitrate ($AgNO_3$) and Zinc Nitrate ($Zn(NO_3)_2.6H_2O$), Ethyl Alcohol (C_2H_5OH), and Congo Red Dye were purchased from SRL Laboratories, Maharashtra, India. The fungus strains used for the study were obtained from the Microbial Type Culture Collection (MTCC, India). The fungus strains used in the study are Candida albicans (MTCC No.183) and Aspergillus fumigatus (MTCC No.9657). Double distilled water was used for all experimental work.

2.2 Methodology:

a) Preparation of extract

The fresh green leaves of Ricinus cummunis plant were washed with double distilled water to remove any attached dirt particles on them. The leaves were then dried in shade and crushed to powder for preparing aqueous extract. The dried powder was boiled in distilled water in the ratio 1:10 (W/V) at 70 degrees on a magnetic stirrer at 1000 RPM for about an hour in the the straw-yellow-coloured solution was then filtered and stored for further use (Parmar et al., 2023).

b) Preparation of Ag-ZnO Nanocomposites

The procedure for preparation of Ag-ZnO nanocomposites is like the one used by Selvan et.al. About 30ml of Ricinus cummunis extract was stirred with 80ml of ethyl alcohol at room temperature on a magnetic stirrer.0.47 g of Zn $(NO_3)_2.6H_2O$ (0.025mol) was added to the above mixture while stirring at 80^0 C for 30 mins. resulting in formation of a white coloured product. About 0.42 g $AgNO_3$ (0.025mol) was added to this solution with continuous stirring at 500 RPM for 30mins. The grey coloured product is then filtered and washed 3-4 times with ethanol and finally dried at 80^0 C for 2-3 hours in a hot air oven (Arumai Selvan et al., 2021a)

c) Characterisation of Ag-ZnO Nanocomposite

The primary confirmation of the Ag-ZnO Nanocomposites was done using UV-visible spectrophotometer (Model-UV-1800 Shimadzu). The suspension of Ag-ZnO nanocomposites were used to record readings between 200-800nm. The FT-IR analysis was done using Shimadzu Make FTIR (Model IR Affinity-1S) and the sample was scanned in the range 400 to 2000cm-1. X-Ray Diffraction pattern (XRD) data was obtained using X-Ray Diffractometer (Rigaku, Miniflex-600 Tokyo, Japan) with a scanning speed of 10 deg./min, Cu-K radiation (λ= 1.542) detector and graphite monochromator was employed. To acquire data the powder form of Ag-ZnO nanocomposites was scanned with continuous scan mode through 2 Θ range of 3^0-90^0. HR-TEM was conducted using Jeol, model 2100 plus, Japan operated at 200kv.

d) Photocatalytic Degradation

The catalytic power of the synthesised nanocomposite is determined by reduction of the Congo Red Dye. 20ppm of the Congo Red Dye was treated with 30 mg of the Ag-ZnO nanocomposite and the degradation of the dye was observed in presence of UV radiation using a UV-Vis spectrophotometer. The degradation percentage of the dye is determined using the formula:

Percentage Degradation = $[(A_0-A)/A_0]X\ 100$

Where, A_0=Initial Absorbance, A= Final Absorbance

e) Antifungal studies

For the NCCLS assay (The National Committee for Clinical Laboratory Standards), preparation of the sample as well as the standard solution were done using 1:3 dilution method. Fluconazole was used as the standard antifungal drug. Sterility and growth controls in the presence of DMSO were also included. The plates were then incubated at 37 °C for 48 hours. The amount of growth was measured using plate reader at λ=492nm, [NCCLS document M27-A2]. Percentage inhibition of the extract against all cell line was calculated using the following formula.

Percentage cell survival = (AT-AB) / (AC-AB) X 100

Where,

AT is Absorbance of treated cells (drug), AB is Absorbance of blank (without cell) and
AC signifies Absorbance of control (untreated)
There by,
% cellular growth inhibition = 100-% cell survival
The effects of test compounds were expressed by IC_{50} values calculated from dose response curves.

f) Cytotoxic Effects

For the study of cytotoxicity of Ag-ZnO NPs the chosen cell line was MCF-7. MCF-7 cell culture was used in these experiments were derived from National Centre for Cell Science (NCCS), Pune. Stock cells of this cell line was cultured in DMEM, supplemented with 10% FBS (fetal bovine serum). All cytotoxicity experiments were carried out in 96 microlitre well-plates. 2×10^4 cells/well was added in to each well of 96 well-plates. Cell lines in exponential growth phase were washed, trypsinzed and re-suspended in complete culture media. Cells were seeded at 2 × 10 4 cells / well in 96 well microlitre plate and incubated for 24 hrs during which a partial monolayer form. The cells were then exposed to various concentrations of the test compounds and standard doxorubicin. After 24 hrs, the cytotoxicity data was evaluated by determining absorbance and calculating the correspondent chemical concentrations. Linear regression analysis with 95 % confidence limit and R2 were used to define dose-response curves and to compute the concentration of chemical agents needed to reduce absorbance of the formazan by 50 % (IC50). Percentage cell growth inhibition or percentage cytotoxicity was calculated by following formula:

% Viability = (AT – AB) / (AC – AB) × 100 (1)

Where,
AT is Absorbance of treated cells (drug), AB = Absorbance of blank (only media) and
AC is Absorbance of control (untreated)
There by,

Percentage Cytotoxicity is100 – % cell survival (2)

Antibacterial Activity

III. RESULTS AND DISCUSSION

1) XRD

X-Ray Diffraction pattern of the synthesised nanocomposite gives an idea about the crystallinity and purity of the nanomaterial. The XRD pattern obtained for green synthesised Ag-ZnO nanocomposite is shown in Figure1. There are six prominent peaks and two minor peaks at 2θ angles. 32.08^0, 46.1^0 and 57.3^0 peaks are for ZnO corresponding to crystallographic planes (100), (102), (110) with hexagonal wurtzite structure (JCPDS card number-361451)(Jamdagni et al., 2018). Other peaks at 37.98^0, 44.15^0,64.3^0 and 77.23^0 suggest presence of Ag along with ZnO corresponding to planes (111), (200), (220) and (311). They match well with the standard (JCPDS card number 04–0783) depicting Face centred Cubic structure (FCC) (Rafique et al., 2023). There is a small additional peak at 54.7^0 which is due to the presence of Ag2O along with metallic Ag [JCPDS card No. 76-1393] (Elyamny et al., 2021). The average size determined using Scherrer's equation.

$$D = \frac{k\lambda}{\beta \cos\theta} \quad \text{(i)}$$

was found to be 21.6 nm, where, D is the average crystalline size of the nanoparticles, k is geometric factor (0.9), k is the wavelength of X-ray radiation source and b is the angular FWHM (full width at half maximum) of the XRD peak at the diffraction angle θ.

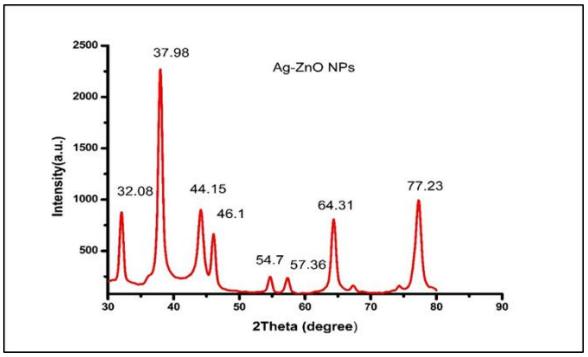

Figure-1 XRD pattern of Ag-ZnO Nanocomposite

2) Infra-Red spectroscopy

The presence of adsorbed molecules and functional groups is determined using FT-IR spectroscopy in the range of $400cm^{-1}$ to $4000cm^{-1}$ (Figure 2). The peaks at $1018cm^{-1}$ and $1149cm^{-1}$ corresponds to stretching frequency of C-N bonds from amine molecules of plant biomass and C-O of ester group respectively (Das & Velusamy, 2014; Varadavenkatesan et al., 2016). A small peak at ~ 1211 cm-1 suggests presence of C-N stretching vibrations The sharp band at 2366cm-1 gives probability of enol of diketones (Biswas et al., 2021). The band at 3900cm-1 is due to the O-H stretching from polyphenols or polysaccharides (Khan et al., 2018).

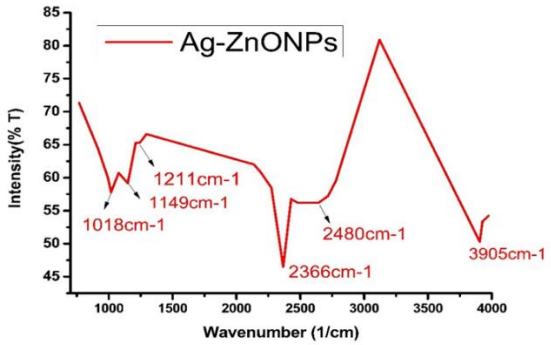

Figure-2 IR spectra of the Ag-ZnO Nanocomposite

3) HR-TEM

The shape size and morphology of the synthesised Nanocomposites can be determined using HR TEM images. The images confirm that the particles are in nano range and most of them are spherical in shape. The average size of the particle being ~60nm. Most of the particles are in in the size range of 30-70 nm. The crystallinity of Ag-ZnO nanocomposites is observed by Selected Area Emission Diffraction pattern (SAED) which suggests polycrystalline nature of the composite (Figure3).

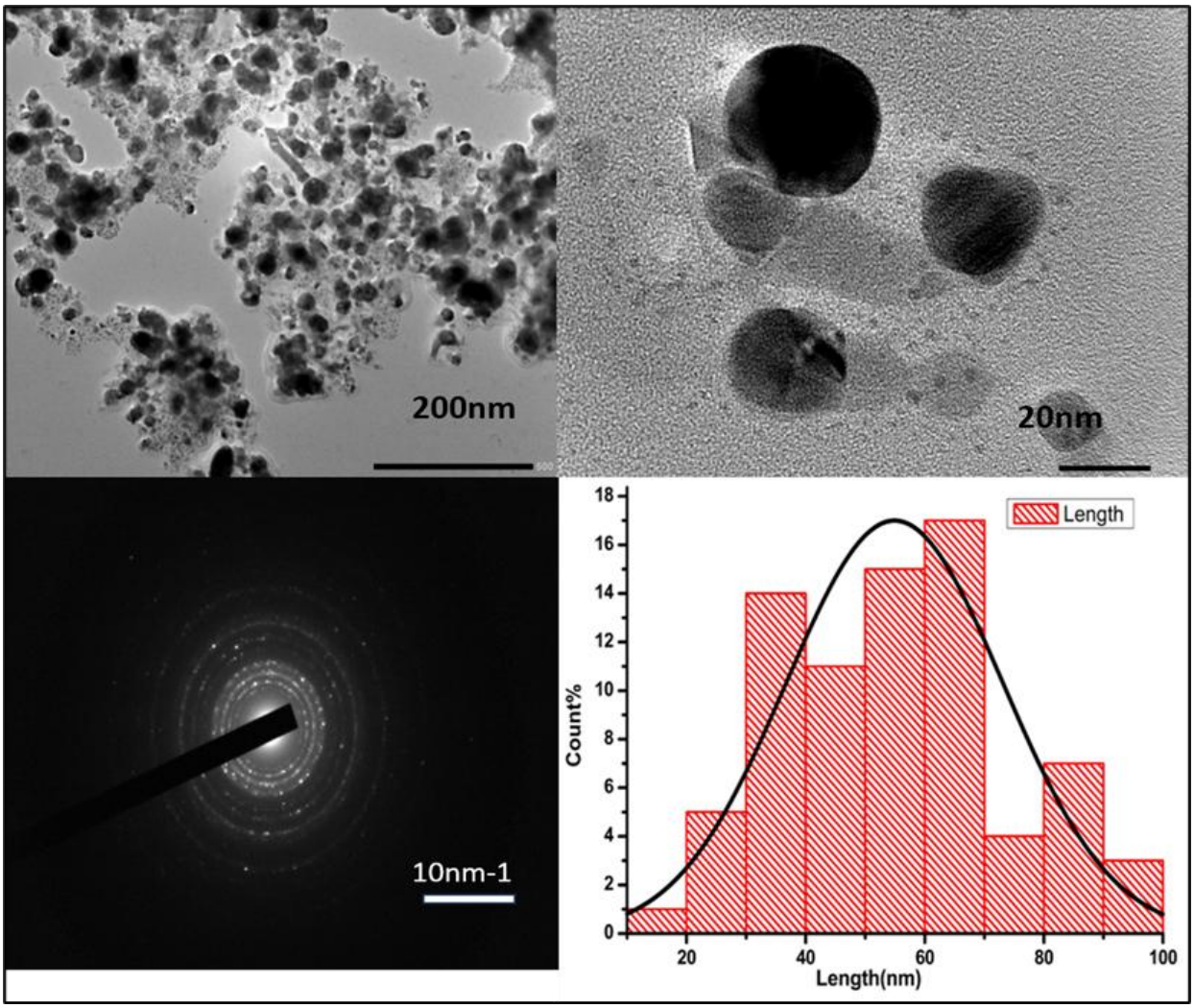

Figure-3: HR-TEM images and histogram revealing size distribution of Ag-ZnO Nanocomposites

4) EDX

The peak at 3 keV confirms the presence of Silver NPs in the sample. The presence of peaks at 1eV,8eV and 9 eV suggests existence of Zn metal in the composite whereas a subsidiary peak at around 0.6 keV points towards presence of Oxygen in the composite. The Weight percentage of Oxygen was found to be 11.21 %, percentage of Zinc was found to be 0.11% and Ag was found to be 88.68%. The distribution of Silver, Zinc and oxygen is showed in Figure 4.

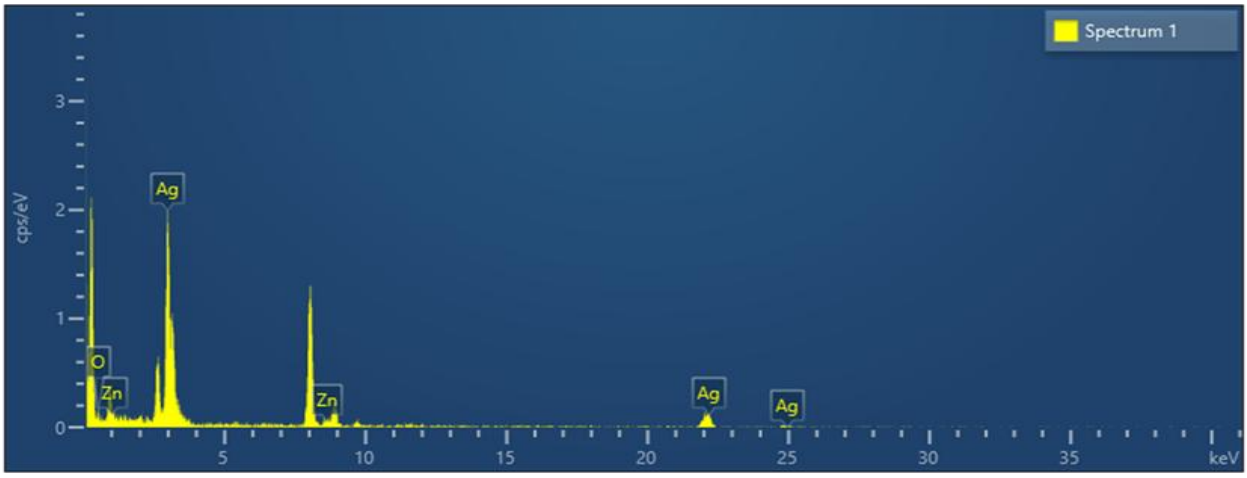

Figure -4: EDX mapping of Ag-ZnO Nanocomposites

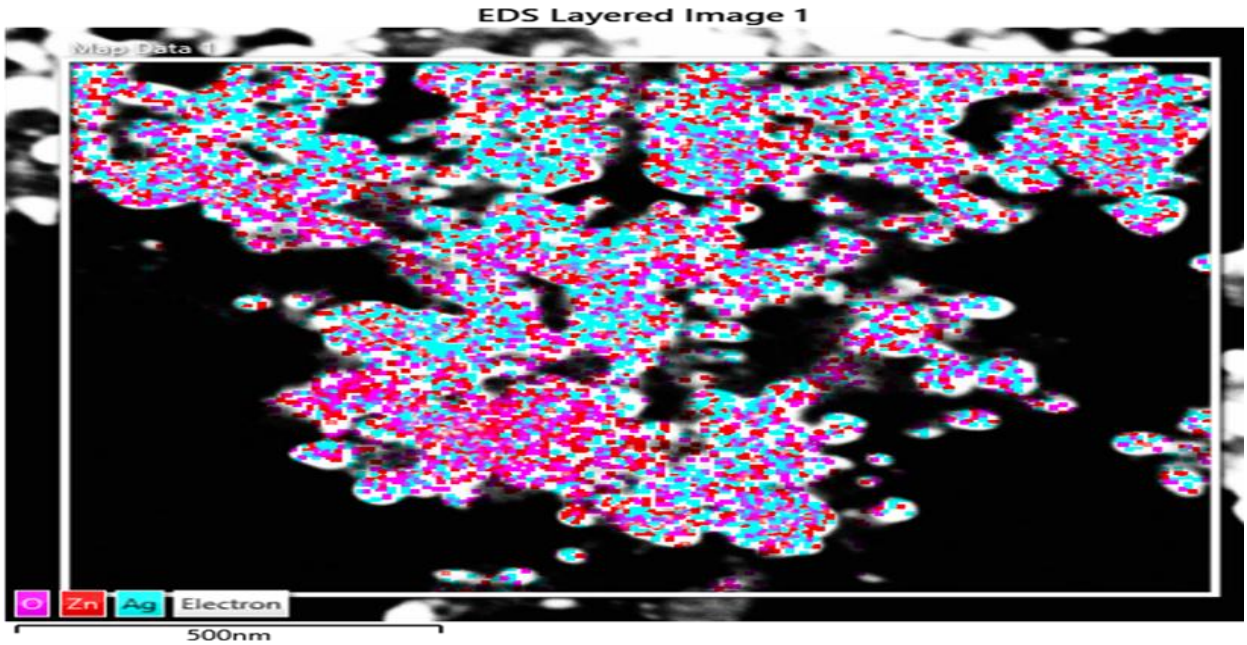

Figure 5- Distribution of Oxygen, Zinc and Silver elements in Ag-ZnO Nanocomposites.

IV. DEGRADATION OF DYE

The photocatalytic effect of the nanosized composite is studied by degradation of anionic azo dye, Congo Red using the composite as the test material. The Congo Red Dye is treated with the prepared Ag-ZnO nanocomposite, and the degradation is observed using UV-VIS spectrophotometer. The Congo Red Dye shows a maximum at 490nm and is profusely used in rubber, textile, paper and plastic industries (Ganapuram et al., 2015).

The expected mechanism of degradation of dyes lies in the fact that a metal nano catalyst when exposed to UV light transfers an electron from the valence band to the conduction band forming an electron-hole pair ($e^- h^+$). The electron-hole pair in turn moves to the surface of the catalyst and reacts with the groups present near the catalyst. The hole reacts with the water molecule to produce hydroxide radical OH^-, and electron reacts with the Oxygen molecule to produce Superoxide anion radical O_2^- (Rauf & Ashraf, 2009). The degradation of the dye molecules can be summarised as follows:

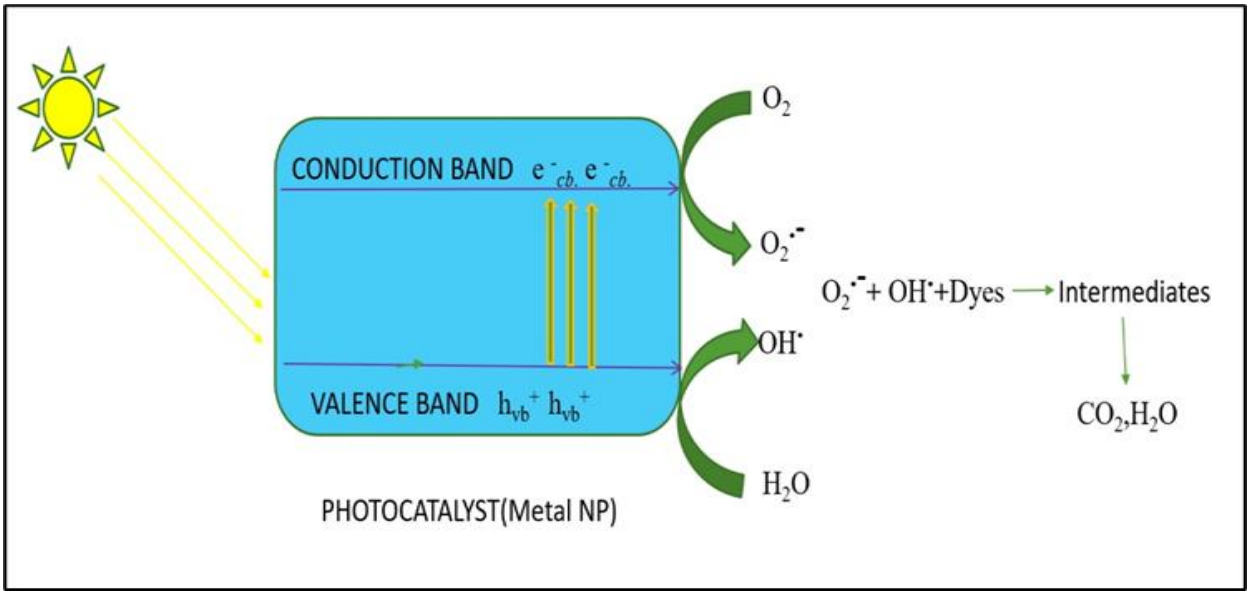

Figure-6: Mechanism of dye degradation

The Congo Red dye is carcinogenic in nature and hence it becomes inevitable to remove it from water bodies. The removal is visually detected initially and then confirmed using spectroscopic data. With the progress in degradation of dye in the solution, the maxima of UV spectra decrease, suggesting a degradation of the dye. The dye solution did not show any change for 24 hours whereas on addition of Ag-ZnO nano catalyst the degradation of CR was observed to be more than 88% within 300 mins (Figure 6a). The plot of $(A_0\text{-}A)/A_0$ vs time is a straight line with $k=0.007021 min^{-1}$ where k denotes rate constant and A_0 and A refers to initial and final absorbance of the dye solution. The nature of the plot confirms the reaction to be of pseudo first order reaction with a corelation factor of 0.9493 (Figure 6b).

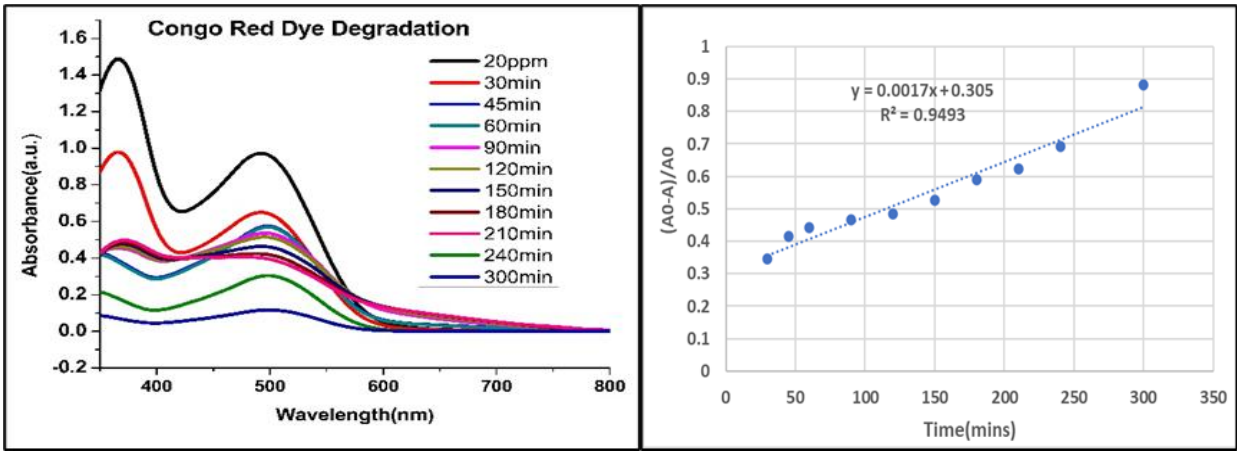

Figure-7a) Decrease in absorbance maxima of CR dye with time b) Plot of $(A_0\text{-}A)/A_0$ vs time

V. ANTIBACTERIAL STUDY

The antibacterial study using 96 well plate is done by observing the change in colour of the sample from pink to blue (Figure 7). The blue colour indicates inhibition whereas pink colour indicates no inhibition of the microbial strain. The MIC for P.aurigunosa is 6.25 µg/ml. using Ag-ZnO as the test compound whereas the MIC for P.aurigunosa using streptomycin is 62.5 µg/ml.The effect of the test compound on S.aurious, E coli and B.subtilis is 50 µg/ml (Table 1).The activity of the standard drug, Streptomycin on these strains

suggests better efficacy of the test compound in case of S. aurious and B. subtilis (Table 2). In case of E. coli bacteria, the standard drug shows better activity.

The mechanism of antibacterial activity of the composite is presumed to be due to penetration of the particles through the cell membrane of the bacterial strain. The difference in results for different bacterial strains is due to the difference in composition of the cell wall which majorly comprises of the layers of peptidoglycan (Mtavangu et al., 2022b).

Sample	Row	1	2	3	4	5	6	7	8	9	10	Bacteria
	µg/ml	0.19	0.39	0.78	1.56	3.125	6.25	12.5	25	50	100	
ZnO - AgNPs	A	-	-	-	-	-	-	-	-	+	++	E. coli
	B	-	-	-	-	-	-	-	-	+	++	E. coli
	C	-	-	-	-	-	-	-	-	+	++	B. subtilis
	D	-	-	-	-	-	-	-	-	+	++	S. aurious
	E	-	-	-	-	-	-	-	-	+	++	B. subtilis
	F	-	-	-	-	-	-	-	+	++	+++	P. aeruginosa
	G	-	-	-	-	-	-	-	-	+	++	S. aurious
	H	-	-	-	-	-	+	++	+++	+++	+++	P. aerigunosa

Table1 Antibacterial studies on B. subtilis, E. Coli, S. aurious and Pseudomonas aeruginosa

Sample	1	2	3	4	5	6	7	8	9	10	Bacteria
µg/ml	1.95	3.90	7.81	15.625	31.25	62.5	125	250	500	1000	
Streptomycin	-	+	++	+++	+++	+++	+++	+++	+++	+++	E. coli
	-	-	-	-	-	+	++	+++	+++	+++	P. aurigunosa
	-	-	-	+	-	-	-	-	+	++	S. aureus
	-	-	-	-	-	-	+	++	+++	+++	B. subtilis

Table2: Antibacterial studies on B. subtilis, E. Coli, S. aurious and Pseudomonas aeruginosa against standard drug Streptomycin.

-No Inhibition (growth found) + Minimum Inhibitory Concentration

++ Minimum Bactericidal Concentration +++ Bactericidal Concentration

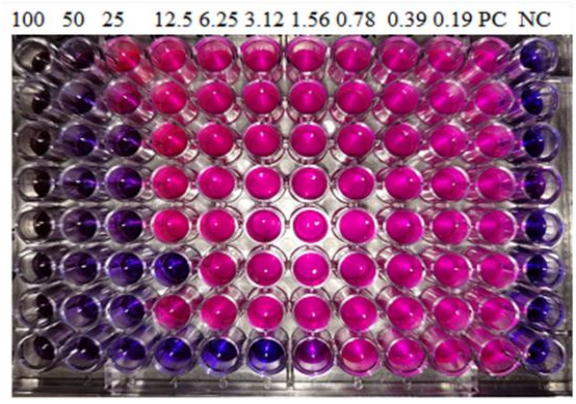

Figure 8: Determination of antibacterial activity on 96-well

VI. ANTIFUNGAL ACTIVITY

Fluconazole is treated as a standard drug and test compounds were tested against the fungal strains Candida albicans and Aspergillus fumigatus in dose dependent manner. End point was determined spectrophotometrically by ELISA plate reader. NCCLS test replicates for anti-fungal activity were analysed every 24 hr for two days to determine the percentage growth inhibition in the presence of the test compound and the standard drug.

Tested compounds were serially diluted in concentration range of 1000 to 1.95 µg/ml in plates with the fungal strain. The working inoculums suspension was added to give final inoculums concentration of 0.5–2.5 X 10^3CFU/ml. The plates were incubated at 37°C for 48 h. The amount of growth was measured using plate reader at λ=450nm. Data were analyzed using Graph pad Prism with use of Dose response curve equation. IC_{50} was derived from curve of % Inhibition V/s Log dose of compound.

Figure 9 reveals the plot of log concentration vs. % cell inhibition of test compounds against Candida albicans. Test compounds show the dose-effect co-relation with maximum linearity with value being 0.9893 and

comparatively lower linearity in case of Candida albicans at value being 0.9264. Activity order of effective compounds can be summarized as below:

Activity report of compounds against Candida albicans

IC_{50} value of Ag-ZnO (IC_{50} value; 71.6µg/ml, R^2= 0.9694) < Fluconazole (IC_{50} value; 108.3µg/ml, R^2= 0.9920). The order of activity suggests that Ag-ZnO NPs are showing significant activity against Candida albicans in comparison to standard drug Fluconazole.

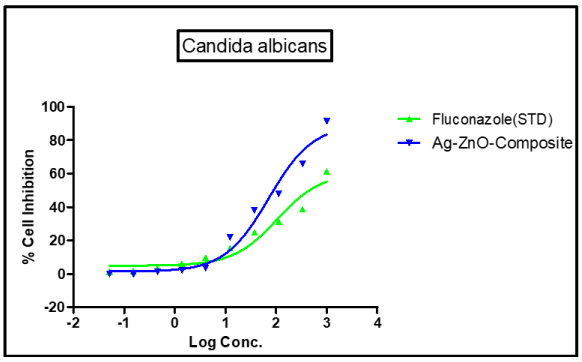

Figure 9: Dose response curve of Test compounds against Candida albicans and Fluconazole

Activity report of compounds against Aspergillus fumigatus

Figure 10 reveals the plot of log concentration vs. % cell inhibition of test compounds against Aspergillus fumigatus. IC_{50} value of Ag-ZnO NPs (IC_{50} value; 132.1 µg/ml, R^2= 0.9921) < Fluconazole (IC_{50} value; 278.7 µg/ml, R^2= 0.9725). The order of activity showed that Ag-ZnO NPs are showing potent activity against Aspergillus fumigatus in comparison to standard drug Fluconazole against Aspergillus fumigatus.

Ag-ZnO NPs(IC_{50} value; 132.1 µg/ml, R^2= 0.9921).

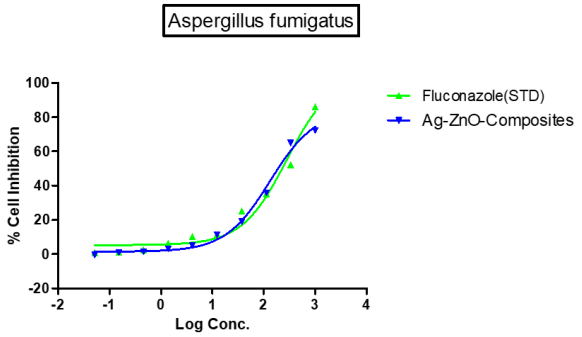

Figure 10: Dose response curve of Test compounds against Aspergillus fumigatus and Fluconazole

Cytotoxic Activities:

In the present investigation, the test compound was tested against MCF-7 cell line. Dose Response Curve (DRC) against all cell lines was plotted with 10 analysis point i.e. with 10 different drug concentrations (Figure 11). The concentration causing 50% cell growth inhibition (IC50) was determined from DRC using GraphPad Prism software (Ver. 5.04) (GraphPad Software, Inc., USA) and Micorsoft Excel 2007 (Microsoft Corporation, USA) application.

Results of tested compounds for MCF-7 cell line are as under:

AgNPS-ZnO (IC_{50} value 16.97µg/ml R2 =0.9849),

Doxorubicin (IC_{50} value 7.197 µg/ml R2 =0.9872)

The results when compared to cytotoxicity of Ag-ZnO Nanocomposites prepared via green synthesis of Murraya koenigii and Zingiber officinale on MCF-7 cell lines (IC_{50}- 30µg/ml and 17.2µg/ml) suggests better efficacy of nanocomposite prepared via Ricinus cumminis (Arumai Selvan et al., 2021b) It is evident from the above results that these nanoparticles show significant anticancer potential. These nanoparticles initiate oxidative stress by production of ROS in cancer cell. The synthesised Nanocomposite when tested against normal cell line i.e Vero, it was found that the IC_{50} value is 236.7µg/ml (Figure-12) which is 100 µg/ml more than the result for MCF-7 cell line)

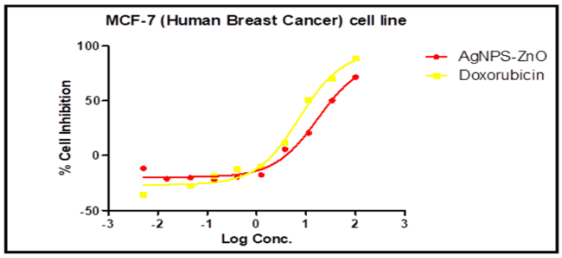

Figure 11: Dose Response curve of various tests against MCF-7 cell line

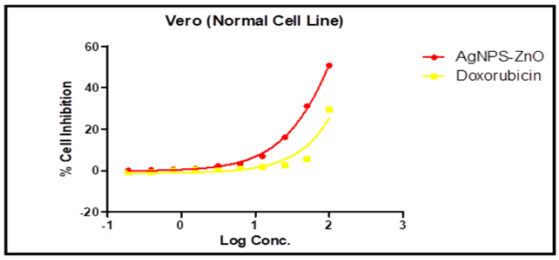

Figure 12: Dose Response curve of various tests against Vero cell line

VII. CONCLUSION

In the present study we have successfully synthesised Ag-ZnO Nanocomposites using aqueous extract of Ricinus cumminis which is confirmed by X-Ray diffraction spectroscopy. The peaks suggest the structure of ZnO as hexagonal wurtzite and Ag as Face centred cubic. IR, EDX spectroscopy and HR-TEM analysis further confirms the size and presence of Zn, Ag and O elements. The prepared nanocomposite is studied for reduction of carcinogenic dye (Congo Red) which is reduced by 88% within 300mins. The biological activity of the synthesised nanocomposite suggests they show better antifungal activity than Ag and ZnO nanoparticles prepared from the aqueous extract of the same plant. The Ag-ZnO nanocomposite also exhibits antibacterial properties against P.aurigunosa, S.aurious, E coli and B.subtilis. The MIC for P.aurigunosa is 6.25 µg/ml, which is better than the effect of standard drug Streptomycin.The MIC for other strains being 50` The analysis of cytotoxic effects of Ag-ZnO nanocomposites suggests significant cytotoxicity against human breast cancer cell (MCF-7) in comparison to standard drug Doxorubicin. Further efficacy of the composite can be explored by studying its cytotoxic effect on other cancer cell lines.

DECLARATION OF ETHICAL STATEMENT

This article does not contain any studies involving animals or human performed by any of the authors.

COMPETING INTERESTS

The authors declare no competing interests.

CONFLICT OF INTEREST

The authors declare no competing interests

FUNDING DECLARATION

No funding has been availed from any external source.

REFERENCES

[1] Ahmad, M., Rehman, W., Khan, M. M., Qureshi, M. T., Gul, A., Haq, S., Ullah, R., Rab, A., & Menaa, F. (2021). Phytogenic fabrication of ZnO and gold decorated ZnO nanoparticles for photocatalytic degradation of Rhodamine B. Journal of Environmental Chemical Engineering, 9(1). https://doi.org/10.1016/j.jece.2020.104725

[2] Akter, M., Sikder, M. T., Rahman, M. M., Ullah, A. K. M. A., Hossain, K. F. B., Banik, S., Hosokawa, T., Saito, T., & Kurasaki, M. (2018). A systematic review on silver nanoparticles-induced cytotoxicity: Physicochemical properties and perspectives. In Journal of Advanced Research (Vol. 9, pp. 1–16). Elsevier B.V. https://doi.org/10.1016/j.jare.2017.10.008

[3] Amiri, M. S., Mohammadzadeh, V., Yazdi, M. E. T., Barani, M., Rahdar, A., & Kyzas, G. Z. (2021). Plant-based gums and mucilages applications in pharmacology and nanomedicine: A review. In Molecules (Vol. 26, Issue 6). MDPI AG. https://doi.org/10.3390/molecules26061770

[4] Arumai Selvan, D. S., keerthi, M., Murugesan, S., Shobana, S., Lakshmi, B., Veena, V., & Rahiman, A. K. (2021a). In vitro cytotoxicity efficacy of phytosynthesized Ag/ZnO nanocomposites using Murraya koenigii and Zingiber officinale extracts. Materials Chemistry and Physics, 272. https://doi.org/10.1016/j.matchemphys.2021.124903

[5] Arumai Selvan, D. S., keerthi, M., Murugesan, S., Shobana, S., Lakshmi, B., Veena, V., & Rahiman, A. K. (2021b). In vitro cytotoxicity efficacy of phytosynthesized Ag/ZnO nanocomposites using Murraya koenigii and Zingiber officinale extracts. Materials Chemistry and Physics, 272. https://doi.org/10.1016/j.matchemphys.2021.124903

[6] Ashna, M., Es-Haghi, A., Karimi Noghondar, M., Al Amara, D., & Yazdi, M. E. T. (2022). Greener synthesis of cerium oxide nanoemulsion using pollen grains of Brassica napus and evaluation of its antitumour and cytotoxicity properties. Materials Technology, 37(8), 525–532. https://doi.org/10.1080/10667857.2020.1863558

[7] Biswas, R., Banerjee, B., Saha, M., Ahmed, I., Mete, S., Patil, R. A., Ma, Y. R., & Haldar, K. K. (2021). Green Approach for the Fabrication of Au/ZnO Nanoflowers: A Catalytic Aspect. Journal of Physical Chemistry C, 125(12), 6619–6631. https://doi.org/10.1021/acs.jpcc.0c10149

[8] Das, J., & Velusamy, P. (2014). Catalytic reduction of methylene blue using biogenic gold

nanoparticles from Sesbania grandiflora L. Journal of the Taiwan Institute of Chemical Engineers, 45(5), 2280–2285. https://doi.org/10.1016/j.jtice.2014.04.005

[9] Elyamny, S., Eltarahony, M., Abu-Serie, M., Nabil, M. M., & Kashyout, A. E. H. B. (2021). One-pot fabrication of Ag @Ag2O core–shell nanostructures for biosafe antimicrobial and antibiofilm applications. Scientific Reports, 11(1). https://doi.org/10.1038/s41598-021-01687-4

[10] Ganapuram, B. R., Alle, M., Dadigala, R., Dasari, A., Maragoni, V., & Guttena, V. (2015). Catalytic reduction of methylene blue and Congo red dyes using green synthesized gold nanoparticles capped by salmalia malabarica gum. International Nano Letters, 5(4), 215–222. https://doi.org/10.1007/s40089-015-0158-3

[11] Haldar, K. K., Biswas, R., Tanwar, S., Sen, T., & Lahtinen, J. (2018). One-Pot Synthesis of Au Embedded ZnO Nanorods Composite Heterostructures with Excellent Photocatalytic Properties. ChemistrySelect, 3(27), 7882–7890. https://doi.org/10.1002/slct.201801234

[12] Hameed, S., Khalil, A. T., Ali, M., Numan, M., Khamlich, S., Shinwari, Z. K., & Maaza, M. (2019). Greener synthesis of ZnO and Ag-ZnO nanoparticles using Silybum marianum for diverse biomedical applications. Nanomedicine, 14(6), 655–673. https://doi.org/10.2217/nnm-2018-0279

[13] Hashemzadeh, M. R., Taghavizadeh Yazdi, M. E., Amiri, M. S., & Mousavi, S. H. (2021). Stem cell therapy in the heart: Biomaterials as a key route. In Tissue and Cell (Vol. 71). Elsevier Ltd. https://doi.org/10.1016/j.tice.2021.101504

[14] Ismail, E., Khamlich, S., Dhlamini, M., & Maaza, M. (2016). Green biosynthesis of ruthenium oxide nanoparticles on nickel foam as electrode material for supercapacitor applications. RSC Advances, 6(90), 86843–86850. https://doi.org/10.1039/c6ra17996g

[15] Jamdagni, P., Khatri, P., & Rana, J. S. (2018). Green synthesis of zinc oxide nanoparticles using flower extract of Nyctanthes arbor-tristis and their antifungal activity. Journal of King Saud University - Science, 30(2), 168–175. https://doi.org/10.1016/j.jksus.2016.10.002

[16] Jena, J., Al-Garni, S., & Gupta, A. K. (n.d.). Ricinus Communis Linn: A Phytopharmacological Review.

[17] Khan, S. A., Noreen, F., Kanwal, S., Iqbal, A., & Hussain, G. (2018). Green synthesis of ZnO and Cu-doped ZnO nanoparticles from leaf extracts of Abutilon indicum, Clerodendrum infortunatum, Clerodendrum inerme and investigation of their biological and photocatalytic activities. Materials Science and Engineering C, 82, 46–59. https://doi.org/10.1016/j.msec.2017.08.071

[18] Kundu, P., Singhania, N., Madras, G., & Ravishankar, N. (2012). ZnO-Au nanohybrids by rapid microwave-assisted synthesis for CO oxidation. Dalton Transactions, 41(29), 8762–8766. https://doi.org/10.1039/c2dt30882g

[19] Mtavangu, S. G., Machunda, R. L., van der Bruggen, B., & Njau, K. N. (2022a). In situ facile green synthesis of Ag–ZnO nanocomposites using Tetradenia riperia leaf extract and its antimicrobial efficacy on water disinfection. Scientific Reports, 12(1). https://doi.org/10.1038/s41598-022-19403-1

[20] Mtavangu, S. G., Machunda, R. L., van der Bruggen, B., & Njau, K. N. (2022b). In situ facile green synthesis of Ag–ZnO nanocomposites using Tetradenia riperia leaf extract and its antimicrobial efficacy on water disinfection. Scientific Reports, 12(1). https://doi.org/10.1038/s41598-022-19403-1

[21] Noohpisheh, Z., Amiri, H., Farhadi, S., & Mohammadi-gholami, A. (2020). Green synthesis of Ag-ZnO nanocomposites using Trigonella foenum-graecum leaf extract and their antibacterial, antifungal, antioxidant and photocatalytic properties. Spectrochimica Acta - Part A: Molecular and Biomolecular Spectroscopy, 240. https://doi.org/10.1016/j.saa.2020.118595

[22] Okumura, M., Fujitani, T., Huang, J., & Ishida, T. (2015). A Career in Catalysis: Masatake Haruta. In ACS Catalysis (Vol. 5, Issue 8, pp. 4699–4707). American Chemical Society. https://doi.org/10.1021/acscatal.5b01122

[23] Ouarez, L., Chelouche, A., Touam, T., Mahiou, R., Djouadi, D., & Potdevin, A. (2018). Au-doped ZnO sol-gel thin films: An experimental investigation on physical and photoluminescence

properties. Journal of Luminescence, 203, 222–229. https://doi.org/10.1016/j.jlumin.2018.06.049

[24] Parmar, M., Arodiya, F., & Sanyal, M. (2023). Green Synthesis of Silver Nanoparticles Using Dry Leaf Extract of Ricinus communis and Its Application in Photocatalytic Degradation of Carcinogenic Dyes and Antifungal Studies. BioNanoScience, 13(2), 450–463. https://doi.org/10.1007/s12668-023-01084-3

[25] Parmar, M., & Sanyal, M. (2022). Extensive study on plant mediated green synthesis of metal nanoparticles and their application for degradation of cationic and anionic dyes. In Environmental Nanotechnology, Monitoring and Management (Vol. 17). Elsevier B.V. https://doi.org/10.1016/j.enmm.2021.100624

[26] Parmar, M., & Sanyal, M. (2024). Biosynthesis of gold nanoparticles using aqueous extract of Ricinus cummunis leaves to augment catalytic degradation of organic dyes and study of its antifungal and antibacterial activities. Particuology, 87, 87–98. https://doi.org/10.1016/j.partic.2023.07.018

[27] Pung, S. Y., Choy, K. L., & Hou, X. (2010). Tip-growth mode and base-growth mode of Au-catalyzed zinc oxide nanowires using chemical vapor deposition technique. Journal of Crystal Growth, 312(14), 2049–2055. https://doi.org/10.1016/j.jcrysgro.2010.03.035

[28] Rafique, S., Bashir, S., Akram, R., Jawaid, S., Bashir, M., Aftab, A., Attique, A., & Awan, S. U. (2023). In vitro anticancer activity and comparative green synthesis of ZnO/Ag nanoparticles by moringa oleifera, mentha piperita, and citrus lemon. Ceramics International, 49(4), 5613–5620. https://doi.org/10.1016/j.ceramint.2022.10.163

[29] Rauf, M. A., & Ashraf, S. S. (2009). Fundamental principles and application of heterogeneous photocatalytic degradation of dyes in solution. In Chemical Engineering Journal (Vol. 151, Issues 1–3, pp. 10–18). https://doi.org/10.1016/j.cej.2009.02.026

[30] Shunmuga Priya, R., Ranjith Kumar, E., Balamurugan, A., & Srinivas, C. (2021). Green synthesized MgFe2O4 ferrites nanoparticles for biomedical applications. Applied Physics A: Materials Science and Processing, 127(7). https://doi.org/10.1007/s00339-021-04699-z

[31] Singh, P. P., Ambika, & Chauhan, S. M. S. (2009). Activity guided isolation of antioxidants from the leaves of Ricinus communis L. Food Chemistry, 114(3), 1069–1072. https://doi.org/10.1016/j.foodchem.2008.10.020

[32] Varadavenkatesan, T., Selvaraj, R., & Vinayagam, R. (2016). Phyto-synthesis of silver nanoparticles from Mussaenda erythrophylla leaf extract and their application in catalytic degradation of methyl orange dye. Journal of Molecular Liquids, 221, 1063–1070. https://doi.org/10.1016/j.molliq.2016.06.064